Kinetic and Structural Analysis of Active Site Mutants of Monofunctional NAD-Dependent 5,10-Methylenetetrahydrofolate Dehydrogenase from *Saccharomyces cerevisiae*†

Wendi Wagner, Andrew P. Breksa III,‡ Arthur F. Monzingo, Dean R. Appling,* and Jon D. Robertus

Institute for Cellular and Molecular Biology, Department of Chemistry and Biochemistry, University of Texas at Austin, Austin, Texas 78712

Received June 1, 2005; Revised Manuscript Received August 1, 2005

ABSTRACT: 5,10-Methylenetetrahydrofolate dehydrogenase (MTD) catalyzes the reversible oxidation of 5,10-methylenetetrahydrofolate to 5,10-methenyltetrahydrofolate. This reaction is critical for the supply of one-carbon units at the required oxidation states for the synthesis of purines and dTMP. For most MTDs, dehydrogenase activity is co-located with a methenyl-THF cyclohydrolase activity as part of bifunctional or trifunctional enzyme. The yeast *Saccharomyces cerevisiae* contains a monofunctional NAD^+-dependent 5,10-methylenetetrahydrofolate dehydrogenase (yMTD). Kinetic, crystallographic, and mutagenesis studies were conducted to identify critical residues in order to gain further insight into the reaction mechanism of this enzyme and its apparent lack of cyclohydrolase activity. Hydride transfer was found to be rate-limiting for the oxidation of methylenetetrahydrofolate by kinetic isotope experiments ($V_H/V_D = 3.3$), and the facial selectivity of the hydride transfer to NAD^+ was determined to be Pro-*R* (A-specific). Model building based on the previously solved structure of yMTD with bound NAD cofactor suggested a possible role for three conserved amino acids in substrate binding or catalysis: Glu121, Cys150, and Thr151. Steady-state kinetic measurements of mutant enzymes demonstrated that Glu121 and Cys150 were essential for dehydrogenase activity, whereas Thr151 allowed some substitution. Our results are consistent with a key role for Glu121 in correctly binding the folate substrate; however, the exact role of C150 is unclear. Single mutants Thr57Lys and Tyr98Gln and double mutant T57K/Y98Q were prepared to test the hypothesis that the lack of cyclohydrolase activity in yMTD was due to the substitution of a conserved Lys/Gln pair found in bifunctional MTDs. Each mutant retained dehydrogenase activity, but no cyclohydrolase activity was detected.

The cofactor tetrahydrofolate (THF)[1] is used in a wide variety of one-carbon metabolic transfers. It can carry one-carbon units in several oxidation states which include 5-methyl (CH_3-THF), 5,10-methylene (CH_2-THF), 5,10-methenyl (CH^+-THF), and 10-formyl (CHO-THF) groups. These groups can be interconverted to meet the metabolic needs of the cell (Figure 1). CH_2-THF makes up an estimated 30% of all cellular folates in mammalian cells (*1*) and sits at the intersection of the folate pathways. 5,10-Methylene-THF dehydrogenase (MTD) catalyzes the reversible oxidation of CH_2-THF to CH^+-THF. In eukaryotes, methylene-THF dehydrogenase activity is typically found in a multifunctional enzyme. Yeast, birds, and mammals contain a

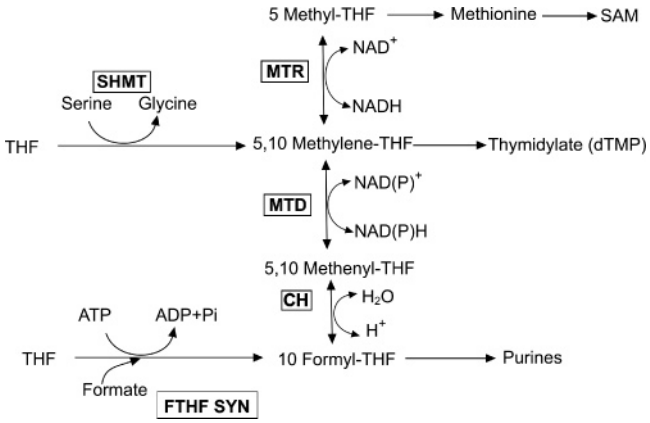

FIGURE 1: The central role of MTD in one-carbon metabolism. One-carbon units are largely brought into the system by the actions of serine hydroxymethyltransferase (SHMT) (EC 2.1.2.1) and 10-formyl-THF synthase (FTHF Syn) (EC 6.3.4.3). Interconversion of the oxidation states of the one-carbon units are mediated by 5,-10-methylene-THF reductase (MTHFR) (EC 1.5.1.20), 5,10-methylene-THF dehydrogenase (MTD), and 5,10-methenyl-THF cyclohydrolase (CH) (EC 3.5.4.9). MTDs are either NADP-dependent (EC 1.5.1.5) or NAD-dependent (EC 1.5.1.15).

† This work was supported by NIH Grant GM 63593, by the Robert A. Welch Foundation, and by the College of Natural Sciences support to the Center for Structural Biology.

* Corresponding author: Department of Chemistry and Biochemistry, 1 University Station A5300, University of Texas at Austin, Austin, TX 78712. Voice, 512-471-5842; fax, 512-471-5849; e-mail, dappling@mail.utexas.edu.

‡ Present address: Western Regional Research Center, Agricultural Research Service, United States Department of Agriculture, 800 Buchanan Street, Albany, CA 94710.

[1] Abbreviations: 2ME, 2-mercaptoethanol; BSA, bovine serum albumin; CH, 5,10-methenyl-THF cyclohydrolase; CH_3-THF, 5-methyltetrahydrofolate; CH_2-THF, 5,10-methylenetetrahydrofolate; CH^+-THF; 5,10-methenyltetrahydrofolate; CHO-THF, 10-formyltetrahydrofolate; MTD, 5,10-methylenetetrahydrofolate dehydrogenase; yMTD, yeast 5,10-methylenetetrahydrofolate dehydrogenase; THF, tetrahydrofolate.

10.1021/bi051038x CCC: $30.25
Published on Web 09/02/2005

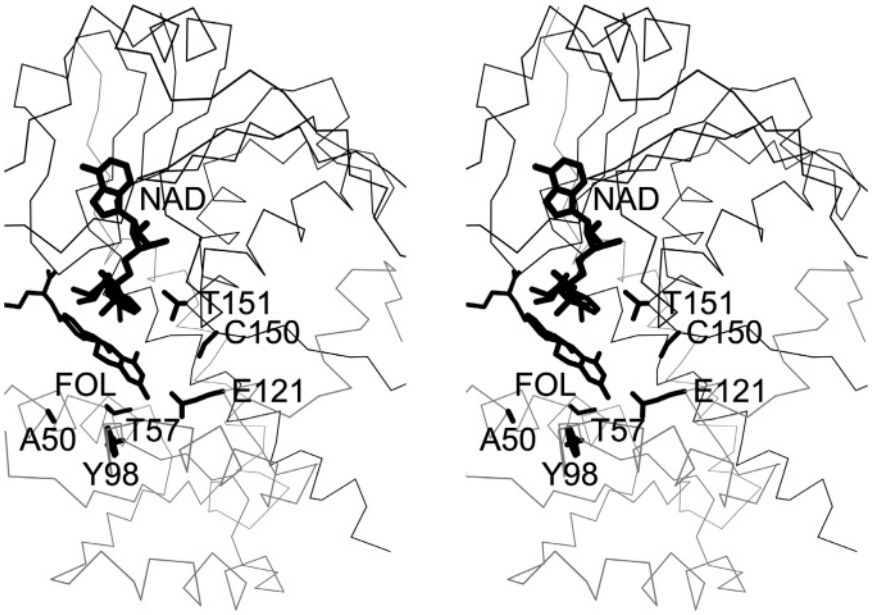

FIGURE 2: Stereogram of the active site of yMTD. The X-ray structure of the yeast MTD−NAD^+ complex was solved by Monzingo et al. (*13*). The closed active site could not accommodate a folate substrate unless the N-terminal domain was rotated about a point near Met64 by 11−16° to superimpose with the corresponding domain of the human enzyme (*15*). The large NAD-binding domain is shown here as a black Cα trace, while the rotated N-terminal domain is shown in lighter gray. The experimentally observed NAD^+ position is shown in thick black bonds, as is a folate analogue (FOL) modeled from the human enzyme. The positions of three conserved residues, E121, C150, and T151, are also shown; their positions rationalize their mutagenic investigation in this study. Three residues have been implicated in cyclohydrolase activity in bifunctional forms of the enzyme. Those positions correspond to A50, T57, and Y98, also shown here.

trifunctional enzyme, called C_1-THF synthase, that also contains methenyl-THF cyclohydrolase and 10-formyl-THF synthetase activities (*2*). The synthetase activity is located in the 70 kDa C-terminal domain, whereas the dehydrogenase and cyclohydrolase activities are located in the 30−35 kDa N-terminal domain. Some mammalian cells express a 34 kDa bifunctional NAD-dependent methylene-THF dehydrogenase/methenyl-THF cyclohydrolase (*3*). The yeast *Saccharomyces cerevisiae* contains a 33 kDa cytoplasmic NAD-dependent 5,10-methylene-THF dehydrogenase (yMTD) (*4*, *5*) in addition to cytoplasmic and mitochondrial trifunctional C_1-THF synthase isozymes (*6*, *7*). However unlike other eukaryotic MTDs, yMTD lacks any appreciable cyclohydrolase activity *in vitro* or *in vivo* and is therefore monofunctional (*4*, *8*). Results obtained from chemical modification studies (*9*−*11*) and from the kinetic comparison of three bifunctional MTDs (*12*) suggest that dehydrogenase and cyclohydrolase activities are co-located in a single active site; however, distinct residues are responsible for the individual activities. Therefore, the alteration of key amino acid residues in the monofunctional yMTD active site may be postulated as the cause for the apparent lack of cyclohydrolase activity. Consistent with this notion, the X-ray crystal structures of yMTD (*13*) and the bifunctional domain of the human trifunctional (*14*) enzymes have been found to be structurally very similar.

After the crystallographic results, two studies have been reported for the bifunctional domain of the human trifunctional enzyme, in which Tyr52, Lys56, Gln100, and Asp125 were identified as critical to both activities (*15*, *16*). Tyr52 (yMTD Tyr53) was implicated in substrate binding; Lys56 (yMTD Thr57) and Gln100 (yMTD Tyr98) were proposed to work together in establishing an environment for hydride transfer, and Lys56 was suggested to participate as a proton acceptor and donor in the cyclohydrolase reaction. Any mutation at Lys56, including K56T, the yMTD (Thr57) equivalent, eliminated cyclohydrolase activity. Likewise, mutations at Gln100 eliminated cyclohydrolase activity, but results for the yMTD equivalent (Tyr98) were not reported. Asp125 (yMTD Glu121) serves in substrate binding, and a carboxylic residue is essential at this position for both activities. Model building based on the X-ray structure of yMTD (*13*) suggests the involvement of two additional highly conserved residues in the dehydrogenase mechanism: Cys150 and Thr151. The positions of these residues, and the previously mentioned Glu121, in the yMTD active site are shown in Figure 2. Finally, we hypothesized that the cyclohydrolase activity of monofunctional yMTD might be restored by substituting Lys for Thr57 and Gln for Tyr98. We report here kinetic, crystallographic, and mutagenesis studies to test this hypothesis and to identify key residues for the dehydrogenase activity in order to gain further insight into the reaction mechanism of this enzyme.

MATERIALS AND METHODS

Materials. Common reagents were high-grade commercial products. NAD^+, NADH, $NADP^+$, NADPH, HEPES, CAPS, MES, Bis-Tris propane, Tris-Cl, and 5-formyl-THF were purchased from Sigma (St. Louis, MO). 2-Mercaptoethanol was purchased from ICN (Costa Mesa, CA) and Triton X-100 from Calbiochem (La Jolla, CA). Formalin-d_2 was purchased from CDN Isotopes (Quebec, Canada). Tetrahydrofolate was prepared by the hydrogenation of folic acid (Sigma) using a PtO_2 catalyst and purification of the THF product on a DEAE cellulose column (Sigma) (*17*, *18*). The preparation of (6*R*,*S*)-CH^+THF from (6*R*,*S*)5-formyl-THF and of (6*R*,*S*)10-formyl-THF from the hydrolysis of (6*R*,*S*)CH^+THF at pH 8.0 were conducted as previously described (*19*). (6*R*,*S*)CH_2THF was prepared from (6*R*,*S*)THF and formaldehyde as previously described (*20*). Yeast alcohol dehydrogenase was purchased

from Calbiochem (La Jolla, CA). Standard 96-well plates (#9017) were purchased from Corning-Costar (Cambridge, MA).

Protein Purification. Wild-type and mutants of the yeast monofunctional cytoplasmic MTD were expressed and purified as previously described (*20*). Protein concentration was determined by a Coomassie dye-binding assay (*21*) using bovine serum albumin (Sigma) as the standard.

Site-Directed Mutagenesis. yMTD plasmid vectors were mutated using the Quik Change Site Directed Mutagenesis kit (Stratagene, La Jolla, CA). Briefly, approximately 10 ng of plasmid and 125 ng of each primer were combined with reaction buffer (100 mM KCl, 100 mM $(NH_4)_2SO_4$, 200 mM Tris-HCl (pH 8.8), 20 mM $MgSO_4$, 1% Triton X-100, and 1 mg/mL BSA), 1 μL of dNTP mix, 2.5 U Pfu DNA polymerase, and sterile deionized water to 50 μL. Reactions were cycled with a denaturing temperature of 95 °C for 30 s, a reannealing temperature of 55 °C for 1 min, and an extension temperature of 68 °C for 10 min for 12−16 cycles on a GeneAmp 2400 (Perkin-Elmer, Norwalk, CT) thermocycler. DpnI (10 U) was added to each reaction and incubated at 37 °C for 1 h to digest the methylated parental strand. One microliter of reaction mixture was then added to 50 μL of *Escherichia coli* XL1-Blue super competent cells and placed on ice for 30 min. Cells were heat-shocked for 45 s at 42 °C, placed on ice for 2 min, and then combined with 500 μL of NZY$^+$ broth (10 g of NZ amine, 5 g of yeast extract, 5 g of NaCl, 12.5 mM $MgCl_2$, 12.5 mM $MgSO_4$, 0.2% glucose, and ddH_2O to 1 L) preheated to 42 °C. Cells were shaken for 1 h, and all 500 μL of solution was plated on LB + ampicillin plates. Plates were incubated at 37 °C overnight and screened for colonies the following morning. Mutants were confirmed by DNA sequencing of the entire insert.

Crystallization. Purified protein less than 2 weeks old was concentrated with Centricon/Centriprep 10 Concentrators (Millipore, Billerica, MA) in the elution buffer (25 mM Tris-HCl, pH 7.6, 2 mM EDTA, 10 mM 2-mercaptoethanol, and 0.2 M KCl) to between 5 and 10 mg/mL. Crystallization of the protein was described previously (*22*), and that procedure was generally followed. The protein was crystallized from 10 to 20% PEG 4000 in 0.1 M Tris-HCl, pH 8.0, at 4 °C in sitting drop conditions. Crystals of the T151A mutant were grown in the additional presence of 5 mM NAD$^+$. Crystals were grown for at least 1 week and data taken within less than 6 weeks.

Data Collection and Processing. Prior to data collection, crystals were treated with cryoprotectant by transfer to artificial mother liquor (20% PEG 4000 and 0.1 M Tris-HCl, pH 8.0) containing increasing amounts of glycerol up to 25% in steps of 5% (5−15 s per step). Crystals, mounted in a nylon cryoloop (Hampton Research, Laguna Niguel, CA), were flash-frozen by dipping in liquid nitrogen and placed in the cold stream on the goniostat.

Diffraction data from crystals of the E121A, C150A, and T151A mutants of yMTD were collected at 105 K with a Mar345 image plate detector (Marresearch GmbH, Norderstedt, Germany) with X-rays generated by a Rigaku RU200 rotating copper anode generator (Molecular Structure Corp., The Woodlands, TX) operated at 50 kV, 100 mA. Diffraction images were processed using DENZO, and data were reduced and scaled using SCALEPACK (*23*).

Structure Determination and Analysis. Molecular replacement for the mutant proteins was performed using wild-type yMTD (PDB accession number 1EDZ) (*13*) as a search model. Molecular replacement solutions were determined using MOLREP (*24*). Refinement of the resulting mutant models was performed with the Crystallography and NMR System (CNS) (version 1.1) (*25*). The geometry of refined models was assessed by PROCHECK (*26*). Computations were done on a Gateway Select SB computer (Poway, CA). Model visualization and rebuilding was done on a Silicon Graphics Indy computer (Mountain View, CA) with the program O (*27*).

5,10-Methylenetetrahydrofolate Dehydrogenase Assay. A cocktail of 2× buffer (166 mM K HEPES, pH 8.0, and 334 mM KCl) and 20 mM NAD$^+$ (stored at −20 °C) was created by mixing 1 vol of each together. 5,10-Methylenetetrahydrofolate (CH_2-THF) was made fresh for each experiment by combining 6 μL of a 1:10 (v/v) dilution of formaldehyde to 500 μL of 10 mM (*6R,S*)THF (stored under vacuum at 4 °C with 500 mM 2-mercaptoethanol). This mixture of formaldehyde and THF was incubated at 37 °C for 5 min and diluted 5-fold with 2.0 mL of deionized water before storing on ice, away from the light. The yield of CH_2-THF from the reaction of formaldehyde and THF was determined by solving the equilibria of THF, formaldehyde, and 2ME (*28*), resulting in a final concentration of 5 mM CH_2-THF stock in 500 mM 2ME.

A microplate assay was used for determination of kinetic parameters of the wild-type and mutant enzymes. Sixty microliters of the cocktail was added to each well of a 96 well microplate. yMTD enzyme was then added along with deionized water to make a final combined volume of enzyme and water of 20 μL. Blanks for each sample were always run, in which acid was added before substrate. Reactions, carried out at 37 °C, were initiated with 20 μL of CH_2-THF diluted with water to 1 mM. Reactions were quenched with 2 vol (200 μL) of 0.36 N HCl after 5 min, and the plate was read at 350 nm on a Molecular Devices Spectramax 190 (Sunnyvale, CA). Blanks were subtracted, and nanomole product was calculated from the absorbance at 350 nm.

For some studies, a continuous fluorescence assay was used. In the fluorescence assay, 600 μL of the desired reaction mixture was placed in a cuvette and the reaction initiated by the addition of 150 μL of the protein sample. The final assay concentrations were identical to those in the 96-well spectrophotometric assay. Samples were excited at 340 nm, and emission was read at 450 nm on a photon-counting spectrofluorometer (model 8000, SLM Instruments, Inc., Urbana, IL). The production of NADH was monitored for 45 s, and the data from 15 to 30 s was used to determine velocities. Initial velocities were calculated from the slope of the plot of nanomoles of NADH produced versus time. Kinetic constants were determined in the same manner as described for the 96-well plate assay.

5,10-Methenyltetrahydrofolate Cyclohydrolase Assay. Cyclohydrolase activity was measured as described previously (*4*). Briefly, 0.1 mM 5,10-methenyl-THF was incubated at 30 °C with yMTD in a 100 mM potassium maleate and 20 mM 2ME buffer at pH 7.4. Activity was monitored by observing the decrease in absorbance of the substrate at 355 nm up to 3 h.

Determination of K_m and k_{cat} for Wild-Type and Mutant MTDs. For the determination of kinetic parameters for NAD^+, CH_2-THF was kept in excess at 400 μM; NAD^+ was varied from 0.5 to 20 mM. For determination of CH_2-THF parameters, NAD^+ was kept in excess at 8 mM; CH_2-THF was varied from 80 to 400 μM. The final concentration of protein was 85−268 nM for all enzymes except for T151A, which required micromolar concentrations. Time points were fit using SigmaPlot to determine the slope (V_o).

Product Inhibition Studies. NADH and (6*R*,*S*)CH^+THF were examined as product inhibitors. Four sets of assays were completed, and in each set, the effect on the V_{max} and K_m of the varied substrate by the presence of an inhibitor was measured. To determine the effect of NADH on the V_{max} and K_m for (6*R*,*S*)CH_2THF, (6*R*,*S*)CH_2THF was varied from 0 to 150 μM at a constant NAD^+ concentration of 8 mM in the presence of 0, 0.27, 0.54, 1.09, and 1.64 mM NADH. To determine the effect of NADH on the V_{max} and K_m for NAD^+, NAD^+ was varied from 0 to 8 mM at a constant (6*R*,*S*)CH_2THF concentration of 459 μM in the presence of 0, 0.54, 1.64, and 7.57 mM NADH. Assays were conducted using the 96-well plate method at 25 °C, pH 8.0 (HEPES), with a final protein concentration of 28 nM.

To determine the effect of (6*R*,*S*)CH^+THF on the V_{max} and K_m for (6*R*,*S*)CH_2THF, (6*R*,*S*)CH_2THF was varied from 0 to 150 μM at a constant NAD^+ concentration of 8 mM in the presence of 0, 4, 10, and 15 μM (6*R*,*S*)CH^+THF. To determine the effect of (6*R*,*S*)CH^+THF on the V_{max} and K_m for NAD^+, NAD^+ was varied from 0 to 6 mM at a constant (6*R*,*S*)CH_2THF concentration of 459 μM in the presence of 0, 2.6, and 5.4 μM (6*R*,*S*)CH^+THF. Assays were conducted using the fluorometric method at 25 °C, pH 8.0 (HEPES), with a final dimer enzyme concentration of 14 nM.

For inhibition studies, the values of K_i, K_{is}, or K_{ii} were determined by curve-fitting the substrate−velocity data to the appropriate equation using a nonlinear least-squares procedure in MathCad Plus (Mathsoft, Inc., Cambridge MA). Equations 1 and 2 are for mixed (noncompetitive) and competitive inhibition, respectively (*29*).

$$v = V_{max}[S]/(K_m(1 + [I]/K_{is}) + [S](1 + [I]/K_{ii})) \quad (1)$$

$$v = V_{max}[S]/(K_m(1 + [I]/K_i) + [S]) \quad (2)$$

Other Inhibitor Studies. (6*R*,*S*)10-Formyl-THF, formate, $NADP^+$, and NADPH were also examined as potential inhibitors of yMTD. For (6*R*,*S*)10-formyl-THF inhibition studies, NAD^+ was varied from 0.5 to 8 mM in the presence of 0, 130, or 260 μM (6*R*,*S*)10-formyl-THF at a constant (6*R*,*S*)CH_2THF concentration of 459 μM. For formate inhibition studies, NAD^+ was varied from 0.5 to 8 mM in the presence of 0, 1, or 10 mM formate at a constant (6*R*,*S*)-CH_2THF concentration of 459 μM. For $NADP^+$ and NADPH inhibition studies, NAD^+ and (6*R*,*S*)CH_2THF were at a constant concentration of 2 mM and 459 μM, respectively. $NADP^+$ was varied from 1.0 to 12 mM, and NADPH was varied from 0.6 to 6 mM. For (6*R*,*S*)10-formyl-THF and formate inhibition studies, the fluorometric method was used, and for $NADP^+$ and NADPH inhibition studies, the 96-well plate assay was used. Assays were conducted at 25 °C, pH 8.0 (HEPES).

pH Dependence. The pH dependence of yMTD activity was measured using both NAD^+ and (6*R*,*S*)CH_2THF. These assays were conducted using the continuous fluorometric method at 25 °C with a final dimer enzyme concentration of 14 nM. A tribuffer was prepared for these studies from stock solutions consisting of equal concentrations of CAPS, MES, and Bis-Tris Propane (all at 83.9 mM), containing 168 mM KCl and 33.6 mM 2-mercaptoethanol, adjusted to various pHs. Assays were conducted at pH = 5.5, 6.0, 7.0, 8.0, 9.0, 10.0, and 11.0. NAD^+ was varied from 0.5 to 10 mM at a constant (6*R*,*S*)5,10-methylene-THF concentration of 285 μM. (6*R*,*S*)5,10-Methylene-THF was varied from 2 to 78 μM at a constant NAD^+ concentration of 2 mM.

Kinetic Isotope Effect Using CD_2THF. [Methylene-^{2}H]-(6*R*,*S*)-5,10-methylene-THF [(6*R*,*S*)CD_2THF] was used as the labeled substrate to measure the kinetic isotope effect. (6*R*,*S*)CD_2THF was prepared in the same manner as (6*R*,*S*)5,-10-methylene-THF, described above, but using formalin-D_2 in place of formaldehyde. All assays were conducted using the 96-well plate method at 25 °C, pH 8.0 (HEPES), with a final protein concentration of 55 nM. To determine the effect on V_{max} and K_m when (6*R*,*S*)CD_2THF was used in place of (6*R*,*S*)CH_2THF, four series of assays were completed. The first two used (6*R*,*S*)CD_2THF, and the other two used (6*R*,*S*)-CH_2THF for comparison. To measure V_{max} and K_m when (6*R*,*S*)CD_2THF or (6*R*,*S*)CH_2THF was varied, the NAD^+ concentration was held constant at 2 mM, while the folate substrate was varied from 2 to 150 μM. To measure the effect on V_{max} and K_m when NAD^+ was varied, NAD^+ was varied from 0.125 to 4 mM in the presence of (6*R*,*S*)CH_2THF or (6*R*,*S*)CD_2THF at 150 μM. The pH dependence of the kinetic isotope effect was determined using the continuous fluorometric method at 25 °C with a final dimer enzyme concentration of 14 nM. Assays were conducted at pH = 5.5, 6.0, 7.0, 8.0, 9.0, 10.0, and 11.0. (6*R*,*S*)CD_2THF was varied from 2 to 78 μM at a constant NAD^+ concentration of 2 mM.

Determination of Facial Selectivity of the Hydride Transfer to NAD^+. The facial selectivity of the hydride transfer was determined using a method based on the procedure described by Arnold et al. (*30*). Briefly, NAD^+ was reduced by yMTD using (6*R*,*S*)CD_2THF as the substrate to give labeled NAD^2H. The NAD^2H was then oxidized by acetaldehyde in the presence of yeast alcohol dehydrogenase (an A-stereospecific enzyme), and proton NMR was used to determine if the resulting NAD^+ product retained or lost deuterium at the 4 position. If the product is NAD^+, yMTD has the same facial selectivity as yeast alcohol dehydrogenase. Conversely, if the product is [4-^{2}H]NAD^+, yMTD has the opposite facial selectivity.

The reaction mixture contained 50 μmol of (6*R*,*S*)CD_2-THF (prepared as described above), 10 μmol of NAD^+, 100 μmol sodium arsenate, and 150 μmol Tris-Cl, pH 8.8, in a final volume of 30 mL. The reaction was initiated with the addition of 20 μg of yMTD. After proceeding for 50 min at room temperature, the reaction was terminated with the addition of 1 N LiOH to a final pH of 12. The reaction was placed in a boiling water bath for 90 s to destroy any remaining NAD^+. The reaction was then cooled to room temperature and the pH adjusted to 7 using 1 N HCl. Five hundred microliters of CH_3CHO (neat) and 3 mg of yeast alcohol dehydrogenase were added to the reaction to oxidize NAD^2H. The reaction was monitored at 340 nm, and when

Table 1: Inhibition Studies

varied substrate	inhibitor	K_{is} (μM)	K_{ii} (μM)	inhibition
(6*R*,*S*)CH_2THF	CH^+THF	43 ± 1.0	7.6 ± 0.8	mixed
(6*R*,*S*)CH_2THF	NADH	1600 ± 120	300 ± 13	mixed
NAD^+	CH^+THF	10 ± 0.25	2.4 ± 0.7	mixed
NAD^+	NADH	5600 ± 250	1500 ± 90	mixed
NAD^+	10-formyl-THF	1600 ± 410	600 ± 200	mixed

there was no further decrease in fluorescence, the pH was lowered to 2 with concentrated HNO_3 and the sample lyophilized. The orange residue was redissolved in 1 mL of D_2O and extracted twice with 4 mL of CH_2Cl_2. The sample was dissolved three times in D_2O and lyophilized. The sample was finally dissolved in 500 μL of D_2O and filtered, and ^{1}H NMR spectra were acquired on a Varian 300 MHz NMR with dioxane added as an internal standard. A total of 480 transients were taken.

RESULTS

Kinetic Analysis and Inhibitor Studies of Recombinant yMTD Using the 96-Well and the Continuous Fluorometric Methods. The traditional assay for CH_2-THF dehydrogenase is based on the production of CH^+-THF ($E = 24\,900\ M^{-1}$ at 350 nm) and typically requires relatively large assay volumes ($\geq$0.5 mL) that must be manually transferred into a cuvette for measurement. In an effort to reduce the assay volume and streamline the procedure, a 96-well plate assay was developed. This method required only 300 μL per assay, and the absorbance was directly measured using a plate reader, thus, eliminating the transfer step. The utilization of a multichannel pipet with this method allowed for rapid setup of a complete kinetic series.

While the 96-well plate assay is useful for routine kinetic studies, it could not be used for product inhibition studies when CH^+-THF was examined as a product inhibitor. We found that neither CH_2-THF nor CH^+-THF interfered with the fluorometric measurement of NADH. Following this observation, we developed a continuous fluorometric assay based on the production of NAD(P)H. Both the fluorometric method and the 96-well plate method were linear over a wide range with a detection limit under 0.5 nmol of the product measured. Both methods allowed for the rapid determination of V_{max} and K_m, and the results were quite comparable between the two assays and similar to values obtained by the traditional cuvette assay (*4*).

NADH and (6*R*,*S*)CH^+THF were examined as product inhibitors when either (6*R*,*S*)CH_2THF or NAD^+ was varied. The fluorescence assay was used to measure the effect of (6*R*,*S*)CH^+THF, and the 96-well plate assay was used to measure the effect of NADH. Four sets of assays were completed, and in each case, the data fit best to the equation for mixed inhibition (Table 1). These results are consistent with a random sequential mechanism for yMTD. (6*R*,*S*)10-Formyl-THF, formate, $NADP^+$, and NADPH were also examined as potential inhibitors of yMTD. Formate, $NADP^+$, and NADPH had no effect on activity (data not shown). However, (6*R*,*S*)10-formyl-THF was found to be a mixed inhibitor, affecting both V_{max} and K_m (Table 1).

A kinetic isotope effect was observed using [methylene-^{2}H]-(6*R*,*S*)-5,10-methylene-THF as the deuterated substrate, indicating hydride transfer as the rate-limiting step. yMTD

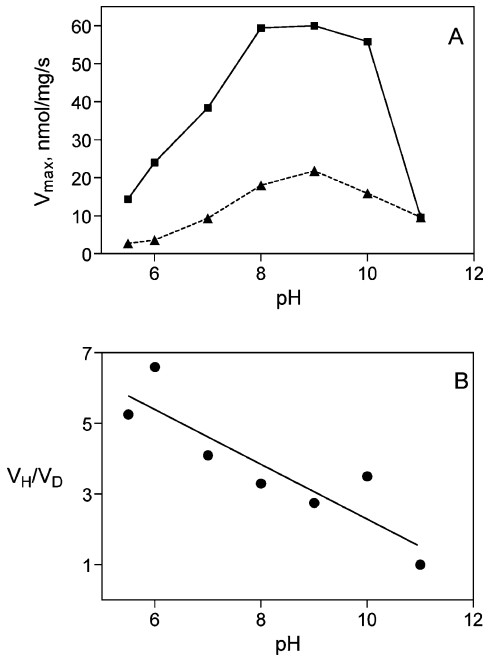

FIGURE 3: pH dependence of kinetic isotope effect. (A) (6*R*,*S*)-CH_2THF (■) or (6*R*,*S*)CD_2THF (▲) was the variable substrate, and NAD^+ was kept at saturating levels. (B) Plot of V_H/V_D (●) vs pH using values derived from data in panel A. Data were acquired using the fluorometric assay at 25 °C, with a final dimer enzyme concentration of 14 nM.

exhibited a V_H/V_D value of 3.3 at pH 8, with $(V/K_m)_H/(V/K_m)_D$ for NAD^+ and (6*R*,*S*)CH_2THF of 7.1 and 3.3, respectively. The pH dependence of yMTD, measured for both NAD^+ and (6*R*,*S*)CH_2THF, was parabolic in shape, with maximal activity exhibited between pH 8 and 10 (Figure 3A). The pH dependence of the kinetic isotope effect was also measured to examine if the rate-determining step or mechanism changed with pH. When V_H/V_D was plotted versus pH, it was found that the isotope effect decreased going from low to high pH (Figure 3B).

The facial selectivity of the hydride transfer was determined using a method based on the procedure described by Arnold et al. (*30*). The ^{1}H NMR spectrum of the NAD produced from [methylene-^{2}H]-(6*R*,*S*)-5,10-methylene-THF after treatment with yeast alcohol dehydrogenase revealed loss of the deuterium (data not shown). Thus, the facial selectivity of the hydride transfer catalyzed by yMTD was the same as yeast alcohol dehydrogenase, Pro-*R*.

Kinetics of Active Site Mutants. Modeling of folate substrates, based on inhibitor complexes observed for bifunctional MTD (*15*), suggested a possible role for three conserved amino acids in substrate binding or catalysis; these are Glu121, Cys150, and Thr151 (Figure 2). Multiple site-directed mutations were made at each of these positions in yMTD. Wild-type yMTD cultures produce about 20 mg/L of media, while the mutants produced from 1 to 10 mg/L. Figure 4 shows the steady-state kinetic assays for wild-type yMTD and several mutants. The parameters derived from these curves are displayed in Table 2. Converting Glu121 to an aspartate (E121D) increased the K_m for NAD^+ by a factor of 2 and increased the K_m for the CH_2-THF substrate more than 5-fold. The k_{cat}, or turnover number, is also decreased about 2-fold; taken together with the K_m data, the E121D mutant exhibits roughly 10% of the wild-type activity.

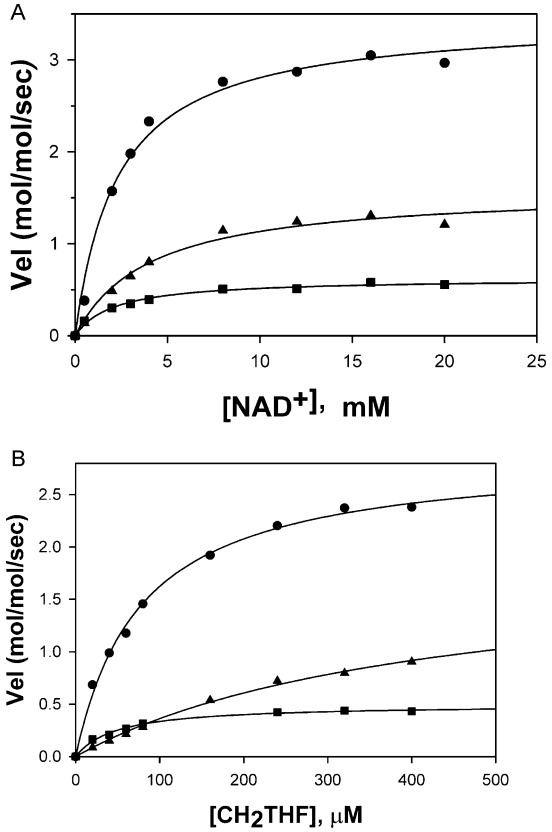

FIGURE 4: Steady-state kinetics of wild-type and mutant yMTDs. WT is shown as circles (●), E121D as triangles (▲), and T151A as squares (■). (A) The kinetics of yMTD as a function of NAD^+ concentration in the presence of saturating concentrations of (6*R*,*S*)-CH_2THF substrate. (B) The kinetics of yMTD as a function of (6*R*,*S*)CH_2THF concentration in the presence of saturating concentrations of NAD^+.

Table 2: Steady-State Kinetic Parameters for Wild-Type and Mutant MTDs

MTD	K_m for (6*R*,*S*)CH_2THF (μM)	K_m for NAD^+ (mM)	k_{cat} ((mol/mol)/sec)	% WT k_{cat}/K_m (CH_2THF activity)
WT	78 ± 5	2.3 ± 0.3	3.2 ± 0.44	100.0%
E121D	418 ± 6	4 ± 0.4	1.7 ± 0.08	10.1%
E121Q	ND[a]	ND[a]	ND[a]	ND[a]
E121A	ND[a]	ND[a]	ND[a]	ND[a]
C150S	ND[a]	ND[a]	ND[a]	ND[a]
C150A	ND[a]	ND[a]	ND[a]	ND[a]
T151A	49 ± 4	2.1 ± 0.3	0.6 ± 0.01	28.1%
T151V	ND[a]	ND[a]	ND[a]	ND[a]

[a] ND, activity not detectable.

When Glu121 was converted to the isosteric glutamine (E121Q) or to alanine (E121A), the enzyme activity dropped to under 1% of wild-type levels and steady-state kinetic parameters could not be accurately assessed with this assay (Table 2).

We made two mutations of Cys150, C150S and C150A. Neither had sufficient residual activity to accurately determine steady-state parameters. A dose−response using increasing amounts of enzyme suggested the C150 mutants had less than 0.25% of wild-type activity (data not shown). We also made two mutations to Thr151, T151V and T151A. The valine mutant had no detectable activity, but the Ala mutant had roughly one-quarter of wild-type activity (Figure 4). It showed a K_m that was 2-fold lower than wild-type for the folate substrate, a K_m identical to the wild-type for NAD^+ but had a 5-fold lower turnover number (Table 2).

X-ray Structure of Active Site Mutants. A concern in interpreting the kinetic behavior of enzyme mutants is that the mutation may have altered the protein structure; it may be that such structural changes, rather than changes in chemical properties, account for the kinetic differences. To test this, we crystallized yMTD mutants with an Ala substituted at each active site position under study and subjected them to X-ray analysis. The X-ray data for E121A, C150A, and T151A are summarized in Table 3. The crystal parameters are similar to those of wild-type, which had space group $P4_12_12$, with a = b = 75.9 Å and c = 160.0 Å (*22*). However, none of the mutant crystals is perfectly isomorphous with the wild-type, and each was phased by molecular replacement. The overall fold of each mutant was very similar to that of wild-type; for example, the Cα positions of the E121A mutant superimposed on those of the wild-type with an rms deviation of 0.78 Å. The electron density maps were of intermediate quality. Figure 5 shows the map in the active site area of the E121A mutant. The density fits the Ala121 side chain perfectly. One would expect that a difference map of the form ($F_{wild-type} - F_{E121A}$) would show density for the side chain beyond the Cβ, and indeed this is so (map not shown). However, the mutant crystal is not perfectly isomorphous with wild-type, and so, the difference density map also shows dozens of other peaks of nearly the same amplitude and volume scattered around the cell. The folding for the C150A and the T151A mutants are also essentially identical to the wild-type, and the main differences are at the site of the point mutations (maps not shown).

Kinetics of Cyclohydrolase Mutations. As mentioned in the Introduction, most MTDs are part of bi- or trifunctional enzymes which include 5,10-methenyl-THF cyclohydrolase activity. When formyl-THF is formed by the 10-formyl-THF synthetase activity (Figure 1), the cyclohydrolase activity catalyzes its conversion to 5,10-methenyl-THF, the substrate for MTD; the cyclohydrolase activity can also be measured in the reverse direction. Yeast MTD lacks the cyclohydrolase activity (*4*), and a comparison with the structure of the N-terminal domain of the human trifunctional enzyme (*14*) was made to rationalize this fact (*13*). Three residues thought to be involved in the binding of water, or in catalysis of the cyclohydrolase reaction, reside in the N-terminal domain of the human enzyme; these are Ser49, Lys56, and Gln100 (*14*). The nucleophilic water is thought to be bound between Ser49 and Gln100, while Lys56 serves to activate the water, presumably by polarizing it toward hydroxide character. The corresponding residues in yMTD are Ala50, Thr57, and Tyr98. These residues were mutated to the human ones singly and in combination, and the cyclohydrolase activity was measured. None of the yMTD mutants produced any cyclohydrolase activity over the buffer-catalyzed rate. We also tested the dehydrogenase activity of these mutants. Converting Thr57 to Lys did not affect the dehydrogenase activity, and converting Ala50 to Ser decreased activity 50%. However, converting Tyr98 to Gln reduced activity more than 30-fold (Table 4).

Table 3: Data Collection and Refinement Statistics for Mutant yMTDs[a]

	E121A	C150A	T151A
space group	$P4_12_12$	$P4_12_12$	$P4_12_12$
cell parameters (Å)	$a = b = 75.8$ $c = 159.8$ $\alpha = \beta = \gamma = 90$	$a = b = 74.24$ $c = 154.08$ $\alpha = \beta = \gamma = 90$	$a = b = 74.8$ $c = 159.8$ $\alpha = \beta = \gamma = 90$
resolution (Å)	2.9	3.8	3.1
R_{merge}	0.078 (0.38)	0.223 (0.55)	0.077 (0.48)
reflections	10833 (1135)	4105 (402)	8332 (811)
$1/\sigma$	18.5 (3.8)	4.2 (2.0)	17.6 (3.5)
completeness (%)	97	82	99
redundancy	4.1	3.0	6.6
$R_{working}$	0.25	0.29	0.24
R_{free}	0.30	0.34	0.30
rmsd bonds	0.009	0.006	0.014
rmsd angles	1.620	1.103	2.521

[a] Values in parentheses are statistics for the last shell.

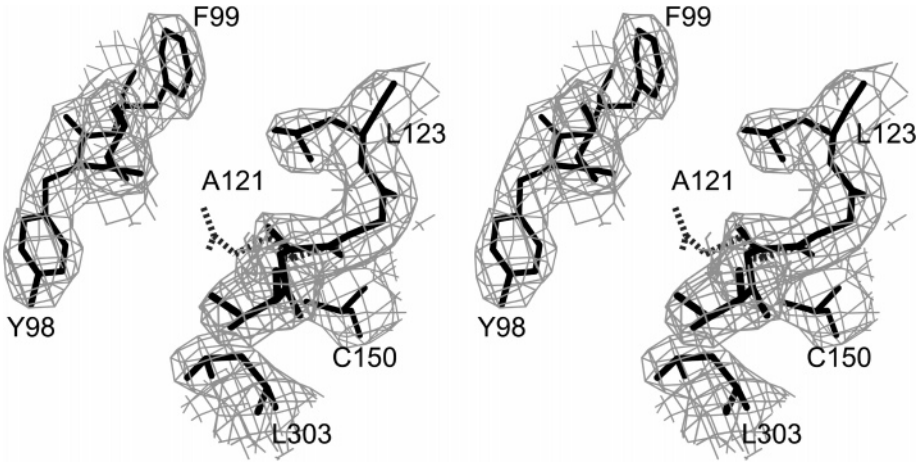

FIGURE 5: Electron density map for the E121A mutant. This stereogram shows electron density centered at the site of the E121A mutation. The map has coefficients of the form $2F_o - F_c$ and is contoured at the 1σ level; the protein bonds are shown as thick black lines. The density for the Ala121 side chain is clearly defined. The position of the E121 residue from the wild-type model is superimposed as a lighter gray-bonded structure; there is clearly no electron density for it in the mutant map.

Table 4: Cyclohydrolase Activity of Mutant yMTDs

protein	cyclohydrolase activity ((nmol/min)/mg)	% wild-type dehydrogenase activity
A50S	ND[a]	45
T57K	ND[a]	100
Y98Q	ND[a]	3
A50S/T57K	ND[a]	100
A50S/Y98Q	ND[a]	8
T57K/Y98Q	ND[a]	2
A50S/T57K/Y98Q	ND[a]	3

[a] ND, activity not detectable.

DISCUSSION

Earlier kinetic studies suggested that the yeast monofunctional MTD proceeds through a sequential reaction mechanism (*4*). Product inhibition studies conducted here are also consistent with a sequential mechanism, in which the order of substrate binding and product release is random. The pH dependence for both substrates was parabolic in shape, with maximal activity exhibited between pH 8 and 10, as previously reported (*4*). A kinetic isotope effect (V_H/V_D) of 3.3 was measured for the oxidation of [methylene-^{2}H]-(6*R*,*S*)-5,10-methylene-THF, indicating that hydride transfer is rate-limiting in the yMTD-catalyzed reaction. This value is similar to the kinetic isotope effects reported for several other 5,-10-methylene-THF dehydrogenases (*12*, *15*). A kinetic isotope effect of 2.5 was determined for the NADP-dependent 5,10-methylene-THF dehydrogenase activity of the yeast cytosolic C_1-THF synthase (data not shown).

The isotope effect (V_H/V_D) was found to be pH dependent, decreasing when going from low to high pH (Figure 3). This observation suggests that, as the pH increases, hydride transfer ceases to be the rate-determining step. Some other step in the reaction, perhaps substrate binding or product release, becomes rate-limiting above pH 10.

The facial selectivity of the hydride transfer to NAD^+ was determined to be Pro-*R* (A-specific). This is the same stereochemical preference exhibited by the $NADP^+$-dependent 5,10-methylene-THF dehydrogenase activity of the cytoplasmic C_1-THF synthase from yeast (*31*). This selectivity is consistent with the orientation of the nicotinamide ring in the yMTD X-ray structure (*13*). The A-side of the ring is facing the open cleft where the folate cofactor binds, positioned to accept the hydrogen from the methylene group.

Efforts to obtain an X-ray structure of the yeast monofunctional MTD in complex with a folate-based substrate analogue have been unsuccessful. However, modeling of such analogues based on inhibitor complexes seen for the human bifunctional MTD (*15*) suggested that three amino acids, conserved in this enzyme family, could be important for substrate binding or catalysis. We made a number of mutations for Glu121, Cys150, and Thr151. Our X-ray

structure suggested that Thr151 contacted the nicotinamide ring of NAD, and we anticipated that mutations at this position would primarily effect the binding of the cofactor. In fact, the K_m for NAD was unaffected by mutation to Ala, the only mutation for which steady-state kinetic data could be measured. The K_m for the CH_2-THF substrate improves slightly, but this 30% change is probably not significant. The major effect of the T151A mutation was on k_{cat}, which decreased more than 5-fold. This could be interpreted as meaning that the smaller methyl side chain causes a minor reorientation of the nicotinamide ring which slightly retards hydride transfer.

We anticipated that Glu121 would be an important active site residue. Although many bifunctional and trifunctional MTDs have an aspartate at this position, the carboxylate is invariant. Our modeling suggested that the longer Glu side chain in the yeast MTD positioned the carboxylate in a similar position to that of the Asp side chain in the human bifunctional enzyme (*15*). The side chain would then be in position to interact with the edge of the pterin ring at N3 and at the exocyclic amine of C2 of the pterin. Such an arrangement is seen in many folate-binding enzymes. Probably, the archetype is the family of dihydrofolate reductases where an invariant carboxylate residue receives hydrogen bonds from N3 and the exocyclic amine of the folate (*32*). When we converted the yeast Glu121 residue to Asp, the dehydrogenase activity was reduced 10-fold (Table 2); the negative charge is conserved, but it is pulled back from the folate substrate. Conversion of Glu121 to the isosteric Gln eliminated any measurable activity, suggesting that the charged species is essential to function. Similar results were reported for the corresponding Asp125 of the DC domain of the human C_1-THF synthase (*16*). The native carboxylate is an excellent hydrogen bond acceptor, while the substituted Gln presents both a hydrogen bond acceptor and a donor at this critical position. This may misalign the folate group slightly, retarding hydride transfer to NAD.

Alternatively, one might speculate that the carboxylate plays a catalytic role in the dehydrogenase reaction. Hydride transfer converts the CH_2-THF to CH^+-THF, which has a formal positive charge at N5 of the pterin. The hydride transfer might therefore be facilitated by electrons being donated into the pterin ring, and a carboxylate would be much better at this function than would an amide. This notion is given support by studies on methylenetetrahydrofolate reductase (MTHFR). Detailed studies showed that Asp120 of MTHFR interacts with the N1−N3 edge of the pterin, similar to that proposed for Glu121 of yeast MTD. Mutation of that Asp to Asn showed that the carboxylate had a role in stabilizing a transient iminium cation at position N5 (*33*).

Cys150 is conserved in many species of MTDs, but is not invariant. The side chain lies in space between those of Glu121 and Thr151, and is in a position to interact with the NAD−folate complex. Its role, if any, in substrate binding or catalysis is unclear. We converted it to Ser, a residue which is a superior hydrogen bond donor and acceptor. The C150S mutant had no detectable activity, nor did an Ala mutant. Replacement of the corresponding cysteine residue (Cys144) with serine in the dehydrogenase/cyclohydrolase domain of the yeast cytoplasmic trifunctional C_1-THF synthase resulted in a 7-fold increase in the K_m for NADP (*34*). Mutation of the corresponding cysteine (Cys147) in the dehydrogenase/cyclohydrolase domain of the human cytoplasmic trifunctional C_1-THF synthase had little or no effect (*15*). The more dramatic effect seen for the C150S mutation in yMTD is difficult to rationalize, but it may be that the bulkier sulfur atom plays a more critical structural role in maintaining active site integrity. We were able to form only poor crystals of the C150A mutant, and they diffracted to only about 4 Å resolution. This is not adequate to make a clear assessment of atomic shifts in the mutant. The poor diffraction and lack of isomorphism with native MTD are consistent with the notion that the structure is perturbed by the mutation.

Our efforts to generate cyclohydrolase activity in yMTD were unsuccessful. We converted three residues thought to be important to that activity, individually and collectively, to the bifunctional active site residues. None of the mutants, including one bearing all three changes, generated convincing cyclohydrolase activity. No doubt, the cyclohydrolase active site has been altered in yeast MTD by other subtle changes which do not allow these residues to be arranged in a useful fashion. Some of the mutations aimed at generating cyclohydrolase activity did affect the dehydrogenase activity. In particular, those proteins in which Y98 was converted to Gln reduced activity 12- to 50-fold (Table 4). It is interesting that when the corresponding Gln in the human bifunctional enzyme was mutated to Ala or Met, cyclohydrolase activity was abolished, but dehydrogenase activity was also decreased to about 20% of wild-type (*16*). This is consistent with the notion that this position may be structurally sensitive, although a molecular rationalization for this observation cannot be made.

It has been proposed that Lys56 of the human bifunctional enzyme, equivalent to position 57 in our yeast structure, was not only involved in cyclohydrolase activity, but also formed a covalent intermediate in the dehydrogenase mechanism (*15*). This is an unlikely proposition since the yeast enzyme, which is clearly a homologue, lacks a Lys at this position; this would seem to eliminate a mechanism with such a particular need. In any case, mutating Thr57 to Lys had no effect on the dehydrogenase activity (Table 4) and confirms that a covalent intermediate between this residue and the folate substrate is not a part of the dehydrogenase mechanism.

ACKNOWLEDGMENT

This work was supported by NIH Grant GM 63593, by the Robert A. Welch Foundation, and by the College of Natural Sciences support to the Center for Structural Biology.

REFERENCES

1. Horne, D. W. (2003) Neither methionine nor nitrous oxide inactivation of methionine synthase affect the concentration of 5,10-methylenetetrahydrofolate in rat liver, *J. Nutr. 133*, 476−478.
2. MacKenzie, R. E. (1984) Biogenesis and interconversion of substituted tetrahydrofolates, in *Folates and Pterins* (Blakley, R. L., and Benkovic, S. L., Eds.) pp 255−306, Wiley, New York.
3. MacKenzie, R. E. (1997) Mitochondrial NAD-dependent methylenetetrahydrofolate dehydrogenase-methenyltetrahydrofolate cyclohydrolase, *Methods Enzymol. 281*, 171−177.
4. Barlowe, C. K., and Appling, D. R. (1990) Isolation and characterization of a novel eukaryotic monofunctional NAD^+-dependent 5,10-methylenetetrahydrofolate dehydrogenase, *Biochemistry 29*, 7089−7094.

5. West, M. G., Barlowe, C. K., and Appling, D. R. (1993) Cloning and characterization of the *Saccharomyces cerevisiae* gene encoding NAD-dependent 5,10-methylenetetrahydrofolate dehydrogenase, *J. Biol. Chem. 268*, 153−160.
6. Staben, C., and Rabinowitz, J. C. (1986) Nucleotide sequence of the *Saccharomyces cerevisiae* ADE3 gene encoding C_1-tetrahydrofolate synthase, *J. Biol. Chem. 261*, 4629−4637.
7. Shannon, K. W., and Rabinowitz, J. C. (1988) Isolation and characterization of the *Saccharomyces cerevisiae* MIS1 gene encoding mitochondrial C_1-tetrahydrofolate synthase, *J. Biol. Chem. 263*, 7717−7725.
8. West, M. G., Horne, D. W., and Appling, D. R. (1996) Metabolic role of cytoplasmic isozymes of 5,10-methylenetetrahydrofolate dehydrogenase in *Saccharomyces cerevisiae*, *Biochemistry 35*, 3122−3132.
9. Schirch, L., Mooz, E. D., and Peterson, D. (1979) Properties of the multifunctional enzyme formyl-methenyl-methylenetetrahydrofolate synthetase (combined) from rabbit liver, in *Chemistry and Biology of Pteridines* (Kisluik, R. L., and Brown, G. M., Eds.) pp 495−500, Elsevier/North-Holland, Amsterdam.
10. Smith, D. D. S., and MacKenzie, R. E. (1983) Methylenetetrahydrofolate dehydrogenase-methenyltetrahydrofolate cyclohydrolase-formyltetrahydrofolate synthetase from porcine liver: evidence to support a common dehydrogenase-cyclohydrolase site, *Can. J. Biochem. Cell Biol. 61*, 1166−1171.
11. Appling, D. R., and Rabinowitz, J. C. (1985) Evidence for overlapping active sites in a multifunctional enzyme: immunochemical and chemical modification studies on C_1-tetrahydrofolate synthase from *Saccharomyces cerevisiae*, *Biochemistry 24*, 3540−3547.
12. Pawelek, P. D., and MacKenzie, R. E. (1998) Methenyltetrahydrofolate cyclohydrolase is rate limiting for the enzymatic conversion of 10-formyltetrahydrofolate to 5,10-methylenetetrahydrofolate in bifunctional dehydrogenase-cyclohydrolase enzymes, *Biochemistry 37*, 1109−1115.
13. Monzingo, A. F., Breksa, A., Ernst, S., Appling, D. R., and Robertus, J. D. (2000) The X-ray structure of the NAD-dependent 5,10-methylenetetrahydrofolate dehydrogenase from *Saccharomyces cerevisiae*, *Protein Sci. 9*, 1374−1381.
14. Allaire, M., Li, Y., Mackenzie, R. E., and Cygler, M. (1998) The 3-D structure of a folate-dependent dehydrogenase/cyclohydrolase bifunctional enzyme at 1.5 Å resolution, *Structure 6*, 173−182.
15. Schmidt, A., Wu, H., MacKenzie, R. E., Chen, V. J., Bewly, J. R., Ray, J. E., Toth, J. E., and Cygler, M. (2000) Structures of three inhibitor complexes provide insight into the reaction mechanism of the human methylenetetrahydrofolate dehydrogenase/cyclohydrolase, *Biochemistry 39*, 6325−6335.
16. Sundararajan, S., and MacKenzie, R. E. (2002) Residues involved in the mechanism of the bifunctional methylenetetrahydrofolate dehydrogenase-cyclohydrolase: the roles of glutamine 100 and aspartate 125, *J. Biol. Chem. 277*, 18703−18709.
17. Blakley, R. L. (1957) The interconversion of serine and glycine: preparation and properties of catalytic derivatives of pteroylglutamic acid, *Biochem. J. 65*, 331−342.
18. Curthoys, N. P., and Rabinowitz, J. C. (1971) Formyltetrahydrofolate synthetase. Binding of adenosine triphosphate and related ligands determined by partition equilibrium, *J. Biol. Chem. 246*, 6942−6952.
19. Rabinowitz, J. C. (1963) Preparation and properties of 5,10-methenyltetrahydrofolic acid and 10-formyltetrahydrofolic acid, *Methods Enzymol. 6*, 814−815.
20. Appling, D. R., and West, M. G. (1997) Monofunctional NAD-dependent, 5,10-methylenetetrahydrofolate dehydrogenase from *Saccharomyces cerevisiae*, *Methods Enzymol. 281*, 178−188.
21. Bradford, M. M. (1976) A rapid and sensitive method for the quantitation of microgram quantities of protein utilizing the principle of protein-dye binding, *Anal. Biochem. 72*, 248−254.
22. Monzingo, A. F., West, M. G., Schelp, E., Appling, D. R., and Robertus, J. D. (1996) Crystallization of the NAD-dependent 5,-10-methylenetetrahydrofolate dehydrogenase from *Saccharomyces cerevisiae*, *Proteins 26*, 481−482.
23. Otwinowski, Z., and Minor, W. (1997) Processing of X-ray diffraction data collected in oscillation mode, *Methods Enzymol. 276*, 307−326.
24. Vagin, A., and Teplyakov, A. (1997) MOLREP: an automated program for molecular replacement, *J. Appl. Crystallogr. 30*, 1022−1025.
25. Brunger, A. T., Adams, P. D., Clore, G. M., DeLano, W. L., Gros, P., Grosse-Kunstleve, R. W., Jiang, J. S., Kuszewski, J., Nilges, M., Pannu, N. S., Read, R. J., Rice, L. M., Simonson, T., and Warren, G. L. (1998) Crystallography & NMR system: a new software suite for macromolecular structure determination, *Acta Crystallogr., Sect. D 54*, 905−921.
26. Laskowski, R. A., MacArthur, M. W., Moss, D. S., and Thornton, J. M. (1993) PROCHECK: a program to check the stereochemical quality of protein structures, *J. Appl. Crystallogr. 26*, 283−291.
27. Jones, T. A., Zou, J. Y., Cowan, S. W., and Kjeldgaard, M. (1991) Improved methods for building protein models in electron density maps and the location of errors in these models, *Acta Crystallogr., Sect. A 47*, 110−119.
28. Kallen, R. G., and Jencks, W. P. (1966) The mechanism of the condensation of formaldehyde with tetrahydrofolic acid, *J. Biol. Chem. 241*, 5851−5863.
29. Cleland, W. W. (1979) Statistical analysis of enzyme kinetic data, *Methods Enzymol. 63*, 103−138.
30. Arnold, L. J., Jr., You, K., Allison, W. S., and Kaplan, N. O. (1976) Determination of the hydride transfer stereospecificity of nicotinamide adenine dinucleotide linked oxidoreductases by proton magnetic resonance, *Biochemistry 15*, 4844−4849.
31. Ramasastri, B. V., and Blakley, R. L. (1964) 5,10-Methylenetetrahydrofolic dehydrogenase from Bakers' yeast. III. Stereospecificity of hydrogen transfer in the reaction catalyzed by the enzyme, *J. Biol. Chem. 239*, 112−114.
32. Reyes, V. M., Sawaya, M. R., Brown, K. A., and Kraut, J. (1995) Isomorphous crystal structures of *Escherichia coli* dihydrofolate reductase complexed with folate, 5-deazafolate, and 5,10-dideazatetrahydrofolate: mechanistic implications, *Biochemistry 34*, 2710−2723.
33. Trimmer, E. E., Ballou, D. P., Ludwig, M. L., and Matthews, R. G. (2001) Folate activation and catalysis in methylenetetrahydrofolate reductase from *Escherichia coli*: roles for aspartate 120 and glutamate 28, *Biochemistry 40*, 6216−6226.
34. Barlowe, C. K., Williams, M. E., Rabinowitz, J. C., and Appling, D. R. (1989) Site-directed mutagenesis of yeast C_1-tetrahydrofolate synthase: analysis of an overlapping active site in a multifunctional enzyme, *Biochemistry 28*, 2099−2106.

BI051038X